Discharge Estimation in a Tidal River with Partially Reverse Flow

Mahmoud F. Maghrebi[1] and Mohammad Givehchi[2]

Abstract: A model for the production of isovel contours in a normalized form, which can be used for estimation of discharge in artificial and natural channels by using a single point of measurement, has been introduced previously by Maghrebi in 2006. Herein, for the first time, application of the model to a tidal river with partially reverse flow, which is caused by opening a sluice gate located asymmetrically close to the right bank of the Ohta floodway in Hiroshima, Japan, is presented. An acoustic Doppler current profiler was used to measure the velocity profiles at different verticals (with several points at each vertical) and then discharge was calculated. In addition, estimated discharge based on each measured point with the aid of the model was obtained. For the measured points away from the low magnitude of isovel values, the predicted discharges are comparable with the measured one. Due to the fluctuations of the measured velocities, instead of a single point of measurement, vertical and horizontal groupings of the measured points were used to estimate the discharge. It is generally proposed to select the measured points from the regions with the corresponding high values of isovels in the range of $u/V<-0.5$ and $u/V>0.5$. The overall results have shown that minimum errors are associated with the horizontal groupings.

DOI: 10.1061/(ASCE)WW.1943-5460.0000049

CE Database subject headings: Tidal currents; River flow; Water discharge.

Author keywords: ADCP; Discharge estimation; Isovel contours; Reverse flow; Tidal river; Couette flow.

Introduction

Discharge measurement in tidal rivers has to be completed quickly, due to the fact that flow conditions vary rapidly. To estimate the discharge accurately, direct measurements are needed. Chen and Chiu (2002) introduced an efficient method to reduce the time and cost of discharge measurement in open channel flows under tidal conditions. Lee and Cheong (2009) used the velocity index and the stage difference height in a multiple regression analysis to establish the stage-discharge curve at a gauging station under tidal current effects. Recently, Kawanisi et al. (2009) have developed an acoustic velocity meter (AVM) in order to monitor long duration of the discharge in real time at a tidal river. They have reported that the agreement between AVM and acoustic Doppler current profiler (ADCP) on water discharge is satisfactory.

On the other hand, the flow characteristics in a recirculation zone are three dimensional. Many experiments have been performed to clarify the flow behavior in the recirculation zone (e.g., Dey and Barbhuiya 2005). Therefore, it is obvious that the flow filed in the recirculation zone of a river under the tidal effect is very complicated.

Observing the time variation of water stage and discharge has shown that during ebb and flood flows the sign of discharge Q will be positive and negative, respectively (Chen and Chiu 2002; Kawanisi 2004). The general form of stage discharge is a looped curve. Meanwhile at a certain time the sign of discharge will be unique. However, the complexity of flow is much higher in a tidal stream with partially reverse flow because in this case, at any time two different regions of flow with positive and negative signs can be discerned. Therefore, to deal with such a complex flow two kinds of tasks should be accomplished. The field measurements should be conducted by a rapid, accurate, and multipoint measurement instrument such as an ADCP. The other task is data processing at the office. A method, which works with a small number of velocity samples, is also required. Maghrebi (2006) has proposed the method of single point measurement for estimation of discharge. A combination of these two will be the solution for describing complicated flow characteristics such as a tidal flow with partially reverse flow. As far as we know, no hypothetical approach is proposed to estimate the discharge in a river with partially reverse flow.

In this paper, for the first time, the flow field with a recirculation zone, as a result of asymmetrically opening a sluice gate is investigated by the model. To be able to apply the model to this case, one has to consider the shear stress as a vector quantity. In the previous applications of Maghrebi model, the river flows were unidirectional.

Cross-Sectional Isovel Contours

The proposed method is able to predict the normalized isovel contours at the cross sections of straight ducts and irregular open channels with different roughness and geometry (Maghrebi and Ball 2006; Maghrebi and Rahimpour 2005). It is assumed that each element of boundary influences the velocity at an arbitrary

[1]Associate Professor, Dept. of Civil Engineering, Ferdowsi Univ. of Mashhad, 91775-1111, Iran. E-mail: Maghrebi@ferdowsi.um.ac.ir

[2]Assistant Professor, Dept. of Civil Engineering, Sistan and Baluchestan Univ., 9816745639, Iran (corresponding author). E-mail: m.givehchi@eng.usb.ac.ir

Note. This manuscript was submitted on June 25, 2009; approved on January 14, 2010; published online on February 4, 2010. Discussion period open until February 1, 2011; separate discussions must be submitted for individual papers. This paper is part of the ***Journal of Waterway, Port, Coastal, and Ocean Engineering***, Vol. 136, No. 5, September 1, 2010. ©ASCE, ISSN 0733-950X/2010/5-266–275/$25.00.

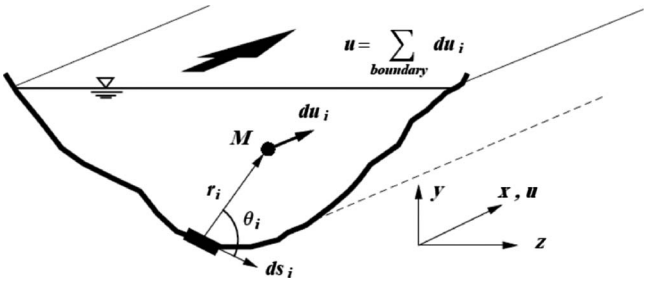

Fig. 1. Illustrative geometry for the effect of boundary roughness on the velocity of an arbitrary point, M, in a river section

point like M on the cross section. Then, the total effect of boundary can be obtained by integration along the wetted perimeter (Fig. 1). It is suggested that

$$\mathbf{u} = \int_{\text{boundary}} c_1 f(\mathbf{r}) \times d\mathbf{s} \tag{1}$$

where $\mathbf{u}$=streamwise velocity vector at a point on the channel section; $f(\mathbf{r})$=velocity function which is similar to the dominant velocity profile over a flat plate with infinite width; $d\mathbf{s}$ =incremental distance along the wetted perimeter; and c_1 =constant related to the boundary roughness. The direction of the velocity vector on the left hand side of Eq. (1) is the same as the vector product of $\mathbf{r} \times d\mathbf{s}$ on the right hand side, which is a normal to flow section toward downstream.

The steady uniform turbulent flow of a fluid in a pipe or in an open channel can be expressed by the power-law velocity distribution as (Chen 1991)

$$\frac{u}{u_*} = c\left(\frac{y}{k_s}\right)^{1/m} \tag{2}$$

where u=streamwise flow velocity; $u_* = \sqrt{\tau_0/\rho}$=boundary shear velocity; τ_0=boundary shear stress; ρ=mass density of fluid; c=coefficient that varies with the global Reynolds number for hydraulically smooth flows or with global relative roughness for fully rough flow; y=normal distance from boundary; k_s =equivalent Nikuradse sand roughness height; and the exponent m usually ranges between 4 and 12 depending on the intensity of turbulence (Yen 2002). However, the sixth root of power-law profile (i.e., $m=6$) has been found to be equal to the Manning's formula, which can be well applied to the natural streams (Chen 1991). In Eq. (2), by replacing radial distance r with y, the following equation will be obtained (Maghrebi 2006):

$$f(\mathbf{r}) = c_2 u_* r^{1/m} \tag{3}$$

where c_2=constant related to the nature of flow. So Eq. (1) can be rewritten as

$$u(z,y) = \int_{\text{boundary}} c_1 c_2 \sin\theta u_* r^{1/m} ds \tag{4}$$

where θ=angle between the positional vector and the boundary elemental vector and $u(z,y)$=local point velocity at an arbitrary position in the channel section. The key point in application of the model to a partially reverse flow is that on the bed region where the flow occurs in opposite directions, the sign of shear stress which is affected by the direction of flow, will be changed. Reverse flow occurs on the left part of the river bed, so the sign of shear stress is negative. On the right boundary as the flow is directed toward downstream, the shear stress has a positive sign. Finally, by using the mean cross-sectional velocity V, the normalized point velocity $\tilde{U}(z,y)$, is given by

$$\tilde{U}(z,y) = \frac{u(z,y)}{V} = \frac{\int_{\text{boundary}} c_1 c_2 \sin\theta u_* r^{1/m} ds}{\frac{1}{A}\int_A \left(\int_{\text{boundary}} c_1 c_2 \sin\theta u_* r^{1/m} ds\right) dA} \tag{5}$$

Eq. (5) provides the normalized velocity at a point as a function of the boundary geometry, relative roughness, and the boundary shear stress distribution. An advantage of Maghrebi's model is that it allows the consideration of the hydraulic characteristics of the boundary and their influences on the flow. Using a single point for velocity measurement in combination with the isovel contours produced by the proposed model, it is easy to estimate the discharge (Maghrebi 2006). The magnitude of normalized corresponding isovel contour passing through a given measured point can be found. The measured velocity at a point in channel cross section is $u(z,y)$ and the magnitude of the normalized corresponding isovel contour is $\tilde{U}(z,y)$, then the total discharge can be obtained by

$$Q_c = A \times \frac{u(z,y)}{\tilde{U}(z,y)} \tag{6}$$

where Q_c=total estimated discharge passing through the cross-sectional area A and $\tilde{U}(z,y) = u(z,y)/V$. When the ratio of $(u/V) = \tilde{U}$ is small, a slight difference in the velocity measurement can lead to a large error in the discharge estimation. The relative percentage of error in discharge estimation is calculated by

$$\text{Error}\% = \frac{Q_a - Q_c}{Q_a} \times 100 \tag{7}$$

where Q_a=actual discharge.

Experimental Application of the Proposed Methodology

All of the previous applications of the proposed methodology have been involved in the unidirectional flows. The correctness of the proposed methodology should be demonstrated when it is applied to a current with two-directional flow. To investigate the results of the methodology, it is applied to a Couette flow between parallel plates with turbulent regime. In the application of the methodology, the key point is to consider positive and negative shear stresses for the plates with positive and negative directions of movement, respectively (Fig. 2).

Let us start with the logarithmic law for the velocity distribution over an infinitely long plate. It is obtained by the use of the Prandtl mixing length hypothesis. For the case of flow over a plate, the mixing length is assumed to be a linear function of the distance from the wall, y, i.e., $l=\kappa y$ where l=mixing length and κ=von Karman constant with a value of 0.4 for clear water.

Velocity distribution between two infinitely long plates, moving in opposite directions each at velocity U with a distance of $2b$ can be found analytically using the same hypothesis. For the case of turbulent Couette flow, the assumption of a parabolic distribution for the mixing length over the distance between two plates is considered as given below

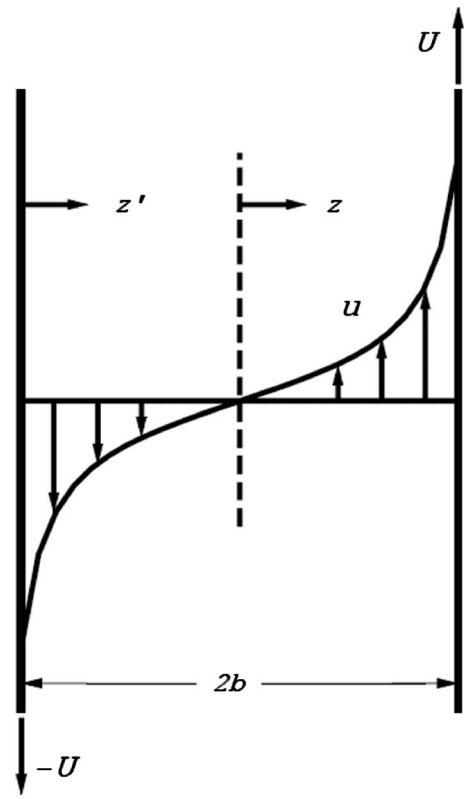

Fig. 2. Coordinates applied for flow between two plates moving in opposite directions

$$l = K(b^2 - z^2) \tag{8}$$

where K=constant and b is one-half of the separation distance and z=distance measured from the centerline between two plates. The velocity distribution is as the following (Spurk 1997):

$$\frac{u(z)}{u_*} = \frac{1}{\kappa}\ln\left(\frac{b+z}{b-z}\right) \tag{9}$$

where u_*=shear velocity. If z' is measured from the wall of the left plate, the velocity distribution of Eq. (9) can be converted to the following form:

$$\frac{u(z')}{u_*} = \frac{1}{\kappa}\ln\left(\frac{z'u_*}{\nu}\right) + \frac{1}{\kappa}\ln\left(\frac{\nu}{2bu_*}\right) \tag{10}$$

where ν=kinematic viscosity of the fluid. From Eq. (10) the velocity distribution in turbulent Couette flow with given Reynolds number defined by $\mathrm{Re}=2bU/\nu$ between the plates can be obtained in the following form:

$$\frac{u(z')}{U} = \frac{u_*2b}{\nu}\frac{\nu}{2bU}\frac{1}{\kappa}\left[\ln\left(\frac{z'}{2b}\right) - \ln\left(1 - \frac{z'}{2b}\right)\right] \tag{11}$$

This equation is plotted schematically in the interval of two plates in Fig. 2.

In Fig. 3 the velocity profiles in Couette flow between two parallel plates moving in opposite directions predicted by Maghrebi's model, Eq. (11), as well as the experimental data (Reichardt 1956, 1959) are shown. The flow is laminar as long as Re $<1{,}500$ and the velocity distribution is then linear. When Re $>1{,}500$, the flow is turbulent. The turbulent velocity profiles are very flat near the center and become very steep near the walls. For laminar flow with Re=1,200, Eq. (11) gives a linear velocity distribution; however, the experimental results and the results produced by Maghrebi's model show some distortion from the linear velocity distribution. For turbulent flow with Re=2,900, good compatibility between the results of Maghrebi's model, Eq. (11), and the experiments can be observed.

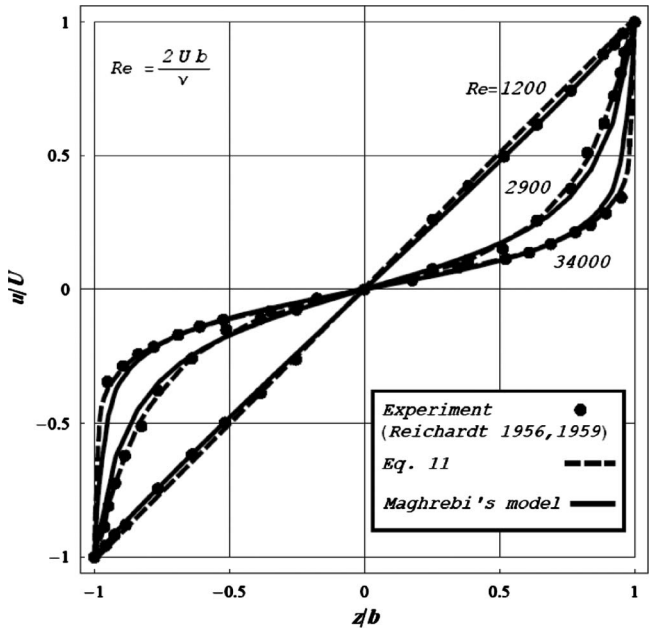

Fig. 3. Normalized velocity profiles in Couette flow between two parallel plates moving in opposite direction

For Re=34,000, where experimental results are available, maximum deviation between the model and experimental results in the range of $-0.95 < z/b < +0.95$ is limited to 12%. However, when closer to the walls, the magnitude of error will be increased considerably and reach 35.8% (Fig. 3).

Study Site and Instrument Description

The Ohta River divides into six branches before discharging into Hiroshima Bay. The Gion diversion channel is a branch of Ohta River [Fig. 4(a)]. At the Gion Bridge location, to control the flow, three sluice gates are installed between the bridge piers. To control the discharge two of the gates (the right and the middle ones when looking downstream) are usually closed. Downstream of the third gate (the one on the right), a recirculation zone is formed [Fig. 4(b)]. The freshwater runoff from the right gate, which is located at about 9 km upstream from the mouth, is limited by fixing the gate opening at a height of 0.3 m from the bottom.

The observation site, which is located at 96 m downstream of the Gion gate, is shown schematically in Fig. 4(b). An ADCP, which was developed by Nortek Inc., was used to accurately measure vertical profiles of mean velocities. The ADCP belongs to a class of acoustic current profilers usually referred to an incoherent Doppler profiler (Lane et al. 1998). The ADCP is operating at 2.0 MHz and 23 Hz pinging rate. It allows one to measure the currents and acoustic scattering strength in depth cell sizes of 0.01 m (Kawanisi 2004). The estimated errors for horizontal and vertical velocity precision are 0.04 and 0.013 m/s, respectively. The directions of ADCP axes (the x-, y-, and z-axes) are based on the definition of a right-handed coordinate system. The x-axis shows the main stream direction, and the streamwise velocity, u,

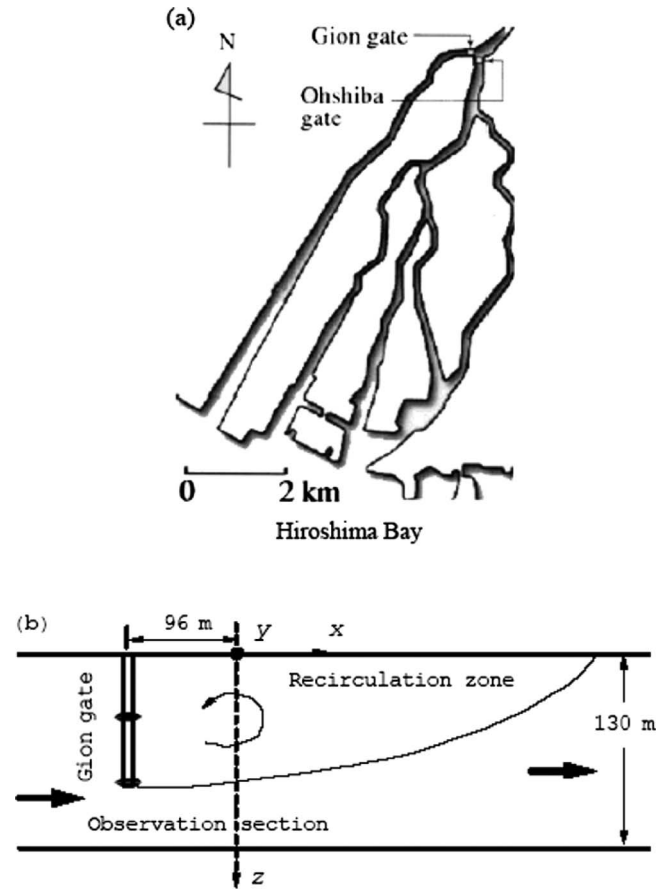

Fig. 4. (a) Ohta estuary; (b) plan view of the observation section

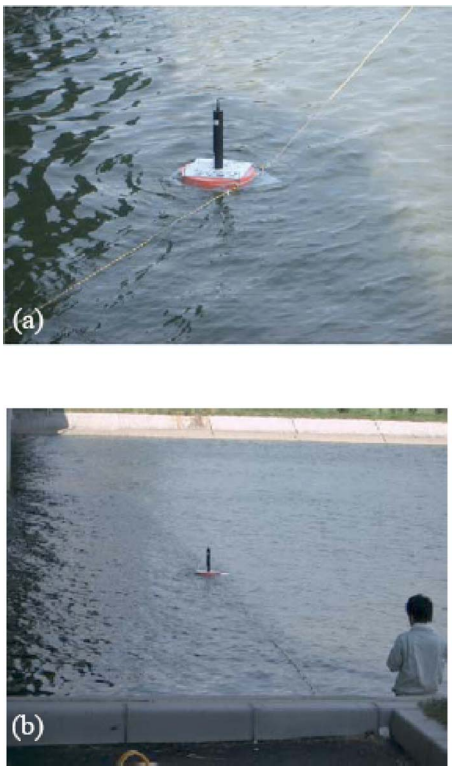

Fig. 5. Moving the ADCP across the Gion diversion channel using a piece of rope: (a) a close view; (b) a far view

is positive during the flood and negative during the ebb. The vertical axis, y, originates at the bottom and points upward.

In order to float the instrument on the water surface, it was placed on a flat and light plate. The supporting system was streamlined to minimize the drag and disturbance. Then a piece of rope was used to move the probe across the river section manually (Fig. 5). The preferred method of measuring discharge in a large tidally influenced stream is the moving-boat method (Rantz 1983; International Organization for Standardization 1979). At each transverse location, the probe was kept stationary for duration of 60 s to collect the instantaneous velocities at a sampling rate of 1 Hz. The measurements have been performed in a round-way recording with the overall time of 32 min. Then the velocity at each point of measurement is obtained by averaging the collected data on two-way recording. Under tidal effects, when the flow characteristics during the gauging can be altered, which means that a simple one-way recording for the measured points is not instantaneous and does not reflect the conditions that existed at the time, a round-way recording is a promising method in discharge measurement in large tidal rivers (Tilley et al. 1999). At the observation site, a number of factors, including position of the Moon, presence of hydraulic structures across the river, variation of the width and depth of river, etc., can affect the magnitude of the acceleration/deceleration. Nevertheless, a quasi-steady approach is adapted to estimate the discharge.

Discharge Estimation

The unsteadiness of flow in a tidal river dictates that the measurements should be completed as soon as possible. To overcome the difficulties of rapid measurements, an ADCP has been used to measure accurate vertical profiles of mean velocity. The water depth was measured using a pressure transducer of ADCP. The bed profile of the measure section is plotted in Fig. 6. The top width of the river at the observation site is about 130 m and the

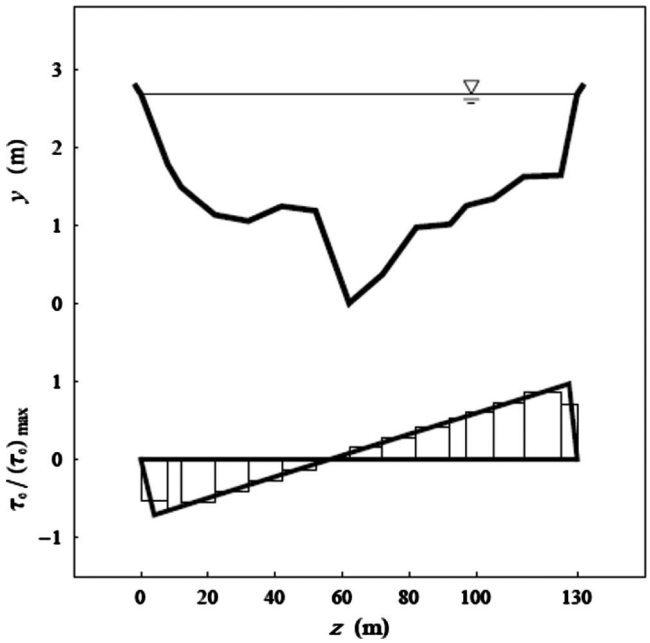

Fig. 6. Observation section of the river bed profile at the immediate downstream of the Gion gate with a simplified shear stress distribution

maximum depth of water is 2.68 m, which is located at a distance of 62 m from the left bank of the river. The measured discharge (called the actual discharge, Q_a) at a river section is estimated by summing up the products of point velocity and the representative area over the entire section.

Accordingly, the mean velocities were measured at different verticals with the transverse distances of 8, 12, 22, 32, 42, 52, 82, 92, 97, 105, 114, and 125 m from the left bank. The cross-sectional area of the river and the average velocity were computed as 194.06 m^2 and 10.7 cm/s, respectively. The corresponding discharge was 20.76 m^3/s. Discharge was also calculated using the energy equation, between upstream and downstream of the sluice gate, at the Gion gate. It was about 20.8 m^3/s, which is slightly larger than the estimated discharge by the aid of ADCP. These measurements are associated with some sources of error. In the application of energy equation, some uncertainties are associated with the measurement of water levels. Also asymmetrical flow through the gate will distort the result. However, it is believed that the overall result using this equation is reliable. On the other hand, the uncertainty of ADCP in the estimation of discharge, which is related to the flow characteristics in the river, is estimated to reach 5%. Continuous water infiltration into the ground from the river bed in the reach of Gion gate and the measured section, quasi-steady assumption of the flow, tidal effects, and errors associated with the measurements by the ADCP can be listed as the main sources of error.

The isovel contours shown in Fig. 7(a) are calculated based on the field data. The velocity on the bed is considered zero and for unmeasured locations, the velocities are extrapolated. As shown, the velocity at the left part of the river section is in the upstream direction, while the flow on the right part flows downstream.

The assumed shear stress distribution which is used to produce the isovel contours from Eq. (5) is shown in Fig. 6. The points of zero shear stress are assumed to coincide with the left and right banks as well as the stagnant region, which is located at an approximate distance of 57 m from the left bank. Then a linear shear stress distribution is applied to the boundary as shown in Fig. 6. The positive shear stresses occur on the right half of the bed profile where the sluice gate is opened and negative values are assumed to occur on the left. The corresponding nondimensional values of the shear stresses for each segment of the wetted perimeter on the bed from left to right are −0.52, −0.63, −0.54, −0.40, −0.27, −0.13, 0, 0.14, 0.28, 0.42, 0.52, 0.61, 0.72, 0.86, and 0.72 (Fig. 6).

The effect of roughness can be accounted by the proposed methodology as can be seen in Eq. (5). Determination of the roughness coefficients in natural rivers is a difficult task. Since the Gion branch of Ohta River is an artificial diversion channel, it is expected that the absolute roughness value along the river cross section to be remained invariant. Our observations from the river section have convinced us about the uniformity of the cross-sectional roughness. Therefore, the assumption of uniform roughness along the wetted perimeter is applied to the methodology. When the distribution of roughness is considered uniform, c_1 in Eq. (5), which is related to roughness value, will be cancelled out from the numerator and denominator.

Fig. 7(b) shows the predicted isovel contours based on the proposed methodology. The isovel contours are calculated by using the bed profile, roughness of bed and simplified shear stress distribution. In Fig. 7, good agreement can be observed between the isovel contours produced by the experimental data and the model.

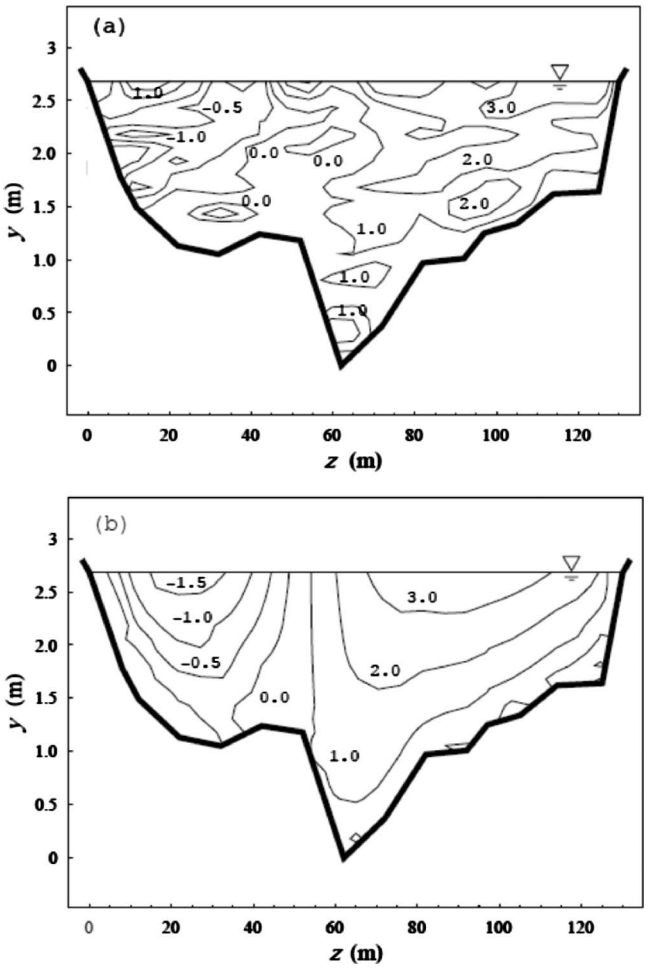

Fig. 7. Isovel counters at the observation section of the Gion River based on (a) field data; (b) Maghrebi's model

Error Analysis

Fig. 8 shows the measured velocity profiles at different verticals with solid dots connected to each other with broken lines. Positive sign for the velocity shows that the direction of flow is toward downstream and negative sign refers to the opposite direction. Due to the probe limitations, velocity could not be measured close to the water surface at a depth of less than 0.2 m and close to the river bed at a vertical distance of less than 10% of the local depth.

Velocity profiles according to the proposed methodology, which are shown with thick solid lines, are plotted against the field data (Fig. 8). Close to the left and right walls of the river, larger differences between the predicted velocity profile and the measured data can be observed. In Fig. 8 the associated errors with the measured velocity points are shown. It is clear that when the normalized isovel contours are close to zero, the estimated discharges by the use of Eq. (5) will approach infinity. These points are near the river bed [Figs. 8(g and l)], near river sides [Figs. 8(a and n)], and near locations where isovel contours show extremely small values [Figs. 8(d and e)] that usually exist in tidal rivers.

Fig. 9 shows the measured velocity profiles along different horizontals with solid dots connected to each other with broken lines. The water depths are 0.2, 0.6, and 1.1 m. Furthermore, velocity profiles according to the proposed model, which are

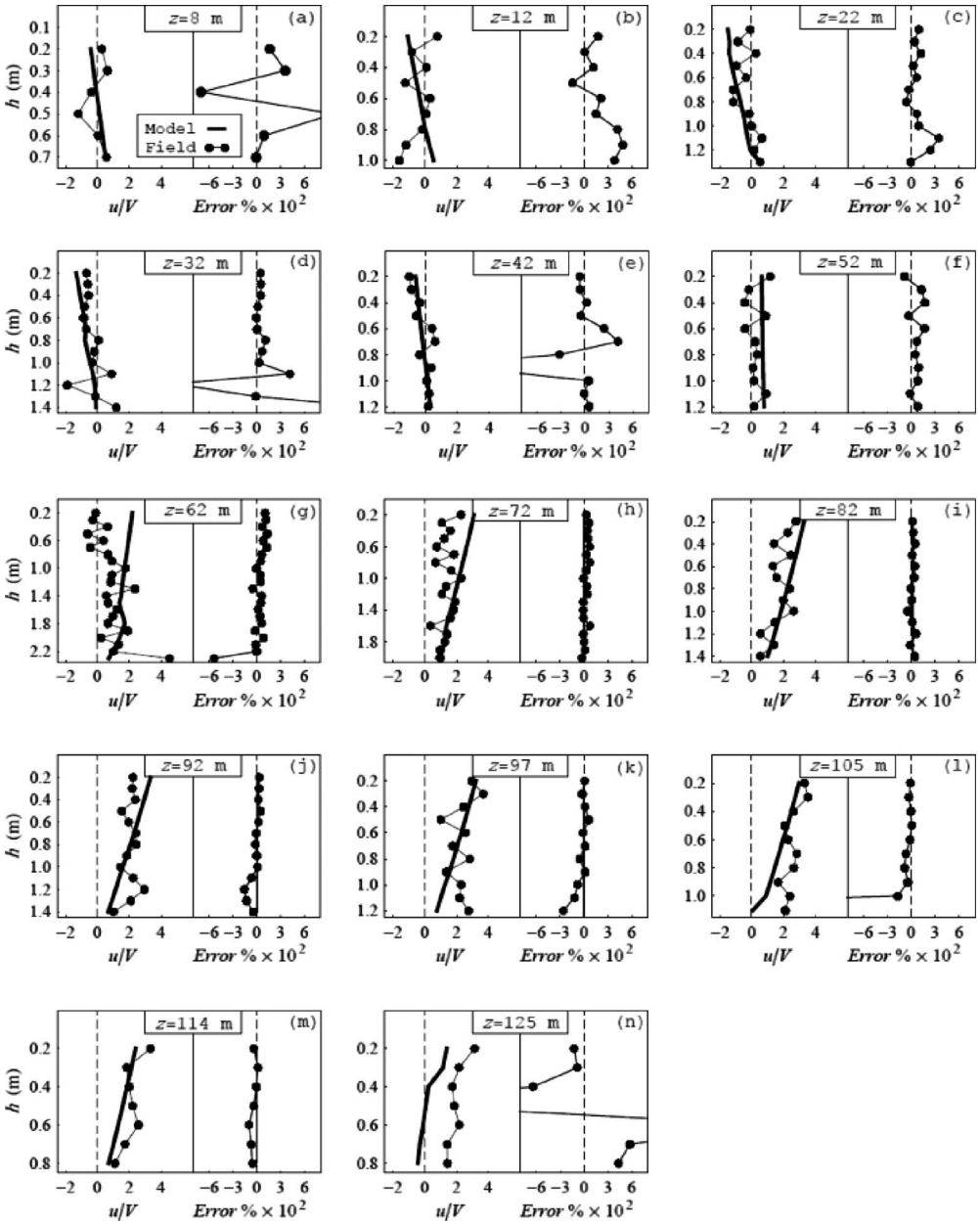

Fig. 8. Measured velocity profiles using ADCP in comparison with the results provided by the proposed model at different transverse verticals of the observation section and the corresponding errors

shown with thick solid lines, are plotted against the field data. In the lower part of the figure, the relative percentage of error in discharge estimation, corresponding with each measured point, is shown.

It is interesting to observe the error distribution as a function of u/V. Fig. 10 shows the results for all 164 points. As expected, as u/V approaches zero, the magnitude of the associated errors, are increased. However, for larger values of $|u/V|$, the magnitude of errors decrease.

In Table 1, for a number of given ranges of u/V, the number of the measured points and corresponding errors of average discharge estimations are given. It is observed that for $u/V<-0.5$ and for $u/V>0.5$, the magnitude of errors are decreased drastically in comparison with the range of $-0.5<u/V<0.5$. This is in accordance with the previously observed results (Maghrebi 2006).

To minimize the uncertainty, it is recommended to estimate the discharge using a number of measured velocity points. Although any combination of the measured points can be used for the estimation of discharge, two ways of grouping are chosen. The first one, shown in Fig. 11(a), seems to be a natural grouping technique because the points in a vertical are measured simultaneously. Based on each point in a group an estimated discharge is obtained. In all cases, the best expected value of discharge will be the mean value. For each column, the number of points contributed in the calculation of the error of average discharge, are given in Table 2. The best results are related to C14 and C9 with random errors of 16.8 and 19.3 %, respectively. C14 is near the right wall and C9 corresponds with the highest velocities at the river cross section.

The differences between real and estimated discharges near the sides of the river and on the left region of the section are relatively larger. It has been mentioned that as the corresponding

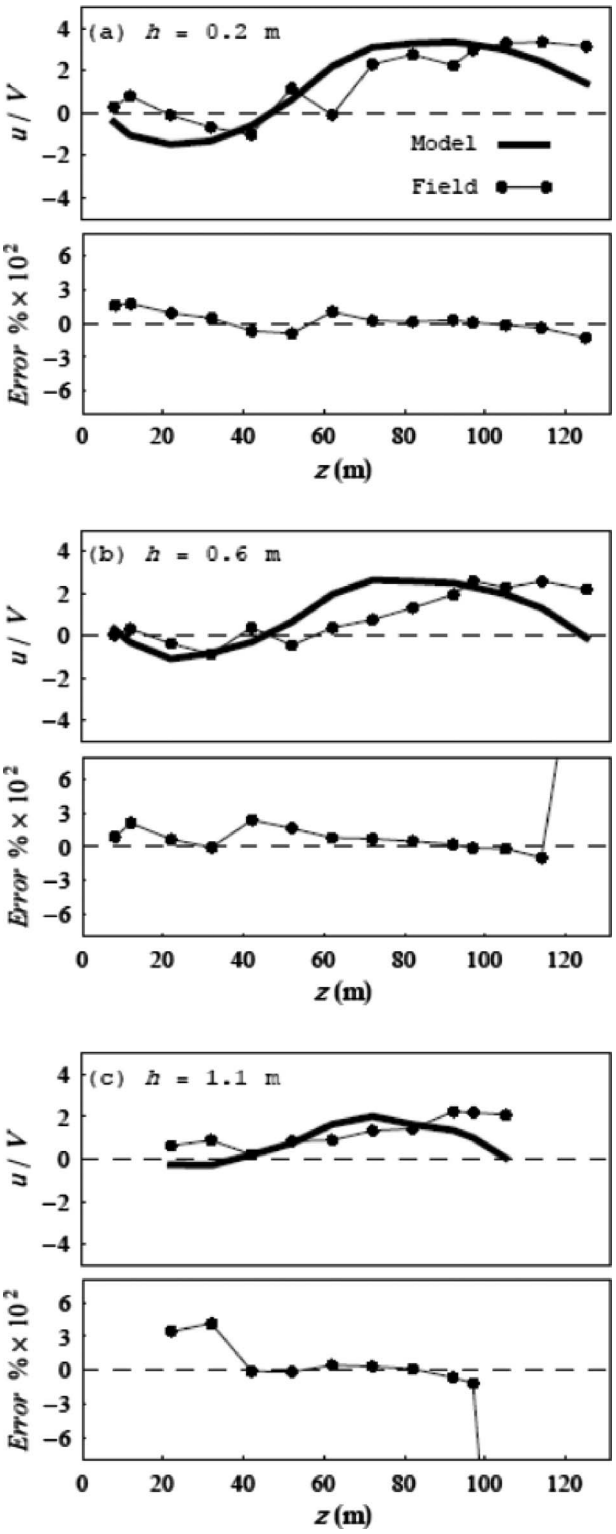

Fig. 9. Measured velocity profiles using ADCP in comparison with the results provided by the proposed model at different transverse horizontals of the observation section and the magnitude of errors

values of the contour lines are increased, errors in average discharge estimation will be decreased (Maghrebi 2006).

The second considered grouping technique for the measured points are shown in Fig. 11(b). These are essentially horizontal arrangements. In Table 3, the errors of average discharge, calculated for this type of grouping, are presented. The number of

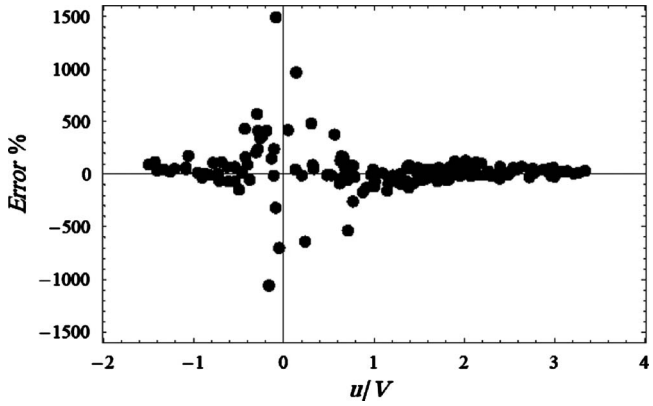

Fig. 10. Variation of error as a function of u/V

horizontal groups reaches 22. The maximum and minimum numbers of measured points contributing to the averaging technique are 14 and 1, respectively.

Unlike the results of vertical grouping (Table 2), the results of horizontal grouping provide a better estimation of discharge (Table 3). Although the measured points in a row are not synchronized, better estimations of average discharges are obtained.

The main reason for this behavior is the higher values of the corresponding isovel contours. Additionally, in a vertical grouping, the presence of the vortical structures, with order of flow depth, produces a significant bias on the measures taken simultaneously; on the contrary, in a horizontal grouping when considering a number of measured points that are not simultaneous, the bias disappears and the errors have a random distribution with an expected value equal to zero. It should be reminded that due to round-way recording the remained bias would be minimized. Consequently, it is believed that this is the main reason of the better results obtained with horizontal groupings.

By discarding some of the points associated with low values of isovel contours, which are shown by gray dots in Fig. 9, the error in the average discharge estimation is generally decreased (Case 2 in Tables 2 and 3). For example, by discarding some of the points in columns C1–C6 and C9–C13 and rows R2–R5, R8–R10, and R12 and R13, the errors are decreased. By considering all 164 measurement points, the error is 0.6 % and by removing the points associated with low values of isovel contours (25 points), error will reach 22%. The results reported herein looks contradictory. It means that by discarding points in the range of

Table 1. Error of Average Discharge Estimation

u/V	Number of points	Error of average discharge (%)
−1.5 to −1.0	9	73.71
−1.0 to −0.5	12	13.20
−0.5 to 0.0	22	239.75
0.0 to 0.5	12	−557.96
0.5 to 1.0	22	−4.88
1.0 to 1.5	21	−28.31
1.5 to 2.0	25	10.28
2.0 to 2.5	19	27.78
2.5 to 3.0	16	29.28
3.0 to 3.5	6	23.56

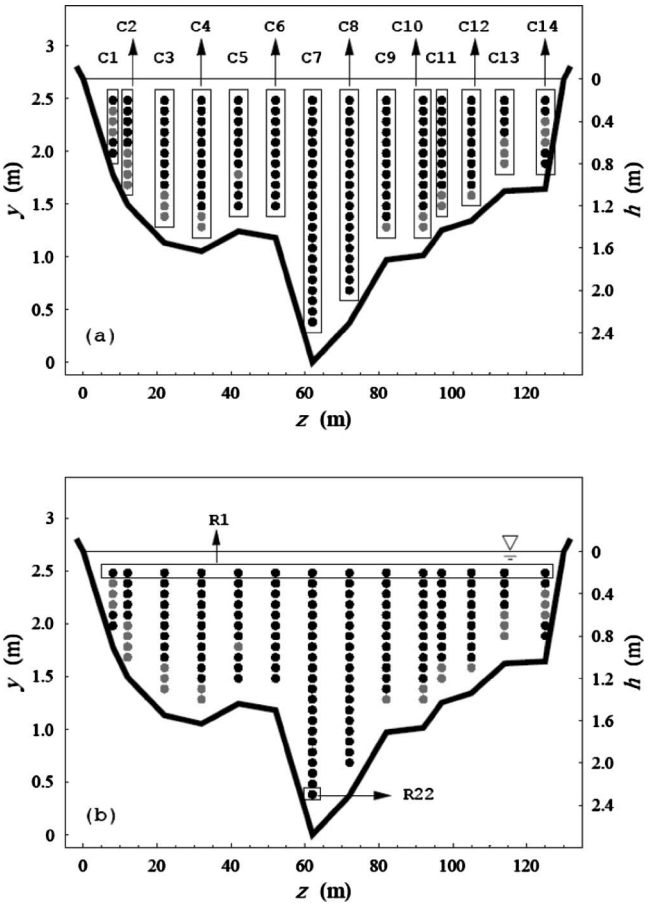

Fig. 11. Definition areas for calculation of the error of average discharge estimation: (a) vertical groups; (b) horizontal groups

$-0.5 < u/V < 0.5$, it is expected to get better results. Observing the errors that correspond with the discarded points shows that the sign of errors for most of the points is negative, which is associated with accidentally increasing the error.

Observation of the errors in estimation of discharge is shown that if at least three points of the measurements are chosen from the higher contour values away from the boundaries at each side of positive and negative contour values, the overall results will be much closer to the actual ones. Each pair of points is selected from the same level. For example, if the points are selected at ($z=32$ m, $h=0.5$ m), (32, 0.6) and (32, 0.7) on the left part of the cross section with negative isovel values and (92, 0.5), (92, 0.6), and (92, 0.7) on the right part of the cross section with positive isovel values, total error will reach 12.3%.

According to Eq. (5), the normalized velocity distributions are sensitive to boundary shear stress distributions. Fig. 12 shows three distributions for the boundary shear stresses and the errors of average discharges. By considering a constant shear stress on bed and zero shear stress on sides, the error in average discharge estimation is 7.6% [Fig. 12(a)]. The error is increased to 17.7% when uniform shear stress distribution is considered [Fig. 10(b)]. Linear shear stress distribution with its maximum values at the river banks is accompanied with a larger error, viz., 115.4% [Fig. 12(c)]. The only difference between this and the one used in this paper (Fig. 6) is the shear stress distribution on the sides of river. Although different shear stress distributions have tangible influences on the predicted discharge, the shear stress distributions plotted in Fig. 12 are the rejected cases in advance and their

Table 2. Errors of Average Discharge Estimation by Using Vertical Groups [Fig. 11(a)]

Vertical groups	z (m)	Number of points (Case 1)	Error of average discharge (%) (Case 1)	Number of points (Case 2)	Error of average discharge (%) (Case 2)
C1	8	6	145.3	3	81.6
C2	12	9	199.9	5	72.8
C3	22	12	81.9	9	45.2
C4	32	13	92.9	11	−25
C5	42	11	−161.2	10	25.8
C6	52	11	64	11	64
C7	62	22	23.6	22	23.6
C8	72	19	25.3	19	25.3
C9	82	13	19.3	12	17
C10	92	13	−20.3	11	−7.8
C11	97	11	−40.2	9	−7.2
C12	105	10	−406.3	9	−46.4
C13	114	7	−42.5	4	−18
C14	125	7	16.8	4	198.7

results are only presented to reveal the sensitivity of the model. In fact, the shear stress distribution given in Fig. 6 is the most realistic distribution. It should be remembered that the pivot point (where the shear stress is assumed to be zero) has a specific location, which can be identified by a rough survey in field data. In this paper, this point is coincided with the zero velocity (stag-

Table 3. Errors of Average Discharge Estimation Using Horizontal Groups [Fig. 11(b)]

Horizontal groups	h (m)	Number of points (Case 1)	Error of average discharge (%) (Case 1)	Number of points (Case 2)	Error of average discharge (%) (Case 2)
R1	0.2	14	24.2	14	24.2
R2	0.3	14	44.8	13	20.7
R3	0.4	14	−48.9	12	54.8
R4	0.5	14	−98.1	12	6.5
R5	0.6	14	232.1	12	80
R6	0.7	14	88	12	96.1
R7	0.8	13	42.2	11	16.6
R8	0.9	11	−115.5	9	30.7
R9	1.0	11	30.1	10	−4.8
R10	1.1	10	−300.6	7	59.1
R11	1.2	9	−105.6	7	−132.9
R12	1.3	6	−37.4	3	−25.3
R13	1.4	5	308.9	2	26.4
R14	1.5	2	22.7	2	22.7
R15	1.6	2	44.7	2	44.7
R16	1.7	2	16.4	2	16.4
R17	1.8	2	31.7	2	31.7
R18	1.9	2	−4.5	2	−4.5
R19	2.0	2	29.7	2	29.7
R20	2.1	1	−10.2	1	−10.2
R21	2.2	1	−2.9	1	−2.9
R22	2.3	1	−536.1	1	−536.1

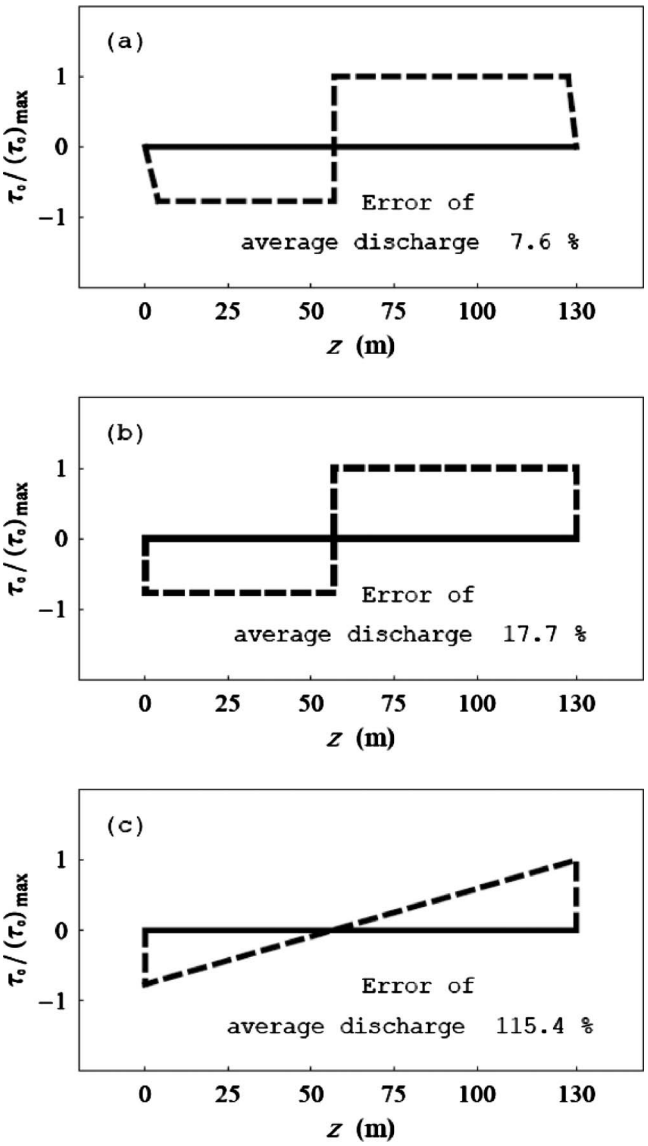

Fig. 12. Sensitivity of the Maghrebi's model to shear stress distribution

nant area) which is resulted from the depth-averaged velocity. The measured discharge by the ADCP and the estimated ones by the proposed methodology as well as the corresponding errors are summarized in Table 4.

Conclusions

In large tidal rivers with partially reverse flow the task of velocity measurement should be completed quickly. This is due to the high unsteadiness of the flow. Rapid measurement maybe fulfilled using an ADCP. Due to the fluctuations of the measured velocities, it is understood that discharge estimation based on a number of measured points would lead to more appropriate results. A combination of a rapid velocity measurement technique and a theoretical approach for estimation of discharge based on minimum number of points of velocity measurements can be considered as an effective way to undertake the task of discharge estimation.

Although no field measurement for estimation of shear stress distribution along the wetted perimeter of the river section (which is needed in the proposed methodology) has been performed, a linear shear stress distribution for complicated circumstances of a tidal river with partially reverse flow and a value of zero at the wall sides seems to be a reasonable assumption.

The results of this study have revealed that the proposed model for estimation of discharge using a single point of velocimetry can be considered as an appropriate, fast and easy model for the production of isovel contours in natural rivers with partially reverse flow. When using a single point of velocity measurement for estimation of discharge, if the related normalized contour values are small, the corresponding errors will be large. Therefore, it is generally proposed to select the measured points from the regions with the corresponding high values of isovels in the range of $u/V<-0.5$ and $u/V>0.5$. It is also suggested that estimation of discharge using horizontal groupings of the points leads to lower magnitude of error in comparison with the vertical groupings.

Table 4. Comparison of the Measured and Calculated Discharges with the Corresponding Errors

	Field data (ADCP)	Model data			
		Fig. 6[a]	Fig. 12(a)[a]	Fig. 12(b)[a]	Fig. 12(c)[a]
Q (m^3/s)	20.76	20.88	22.34	24.43	44.72
Error (%)	—	0.6	7.6	17.7	115.4

[a]Refer to figure for the distribution of shear stress.

Acknowledgments

The writers would like to thank all of the anonymous reviewers. Their comments were appreciated in the revision of the paper.

Notation

The following symbols are used in this paper:

A = cross-sectional area of the stream;
b = one-half of distance between two plates;
c = coefficient;
c_1, c_2 = constants related to the boundary roughness and flow regime, respectively;
$d\mathbf{s}$ = vector notation along the wetted perimeter;
$f(\mathbf{r})$ = velocity function;
h = local depth of flow;
K = constant;
k_s = equivalent Nikuradse sand roughness height;
l = mixing length;
m = denominator in exponent of the power-law velocity distribution;
Q = discharge;
Q_a = measured discharge;
Q_c = calculated discharge;
Re = Reynolds number;
r = radial distance;
$\mathbf{r}$ = positional vector;
U = velocity;
$\tilde{U}(z,y)$ = normalized point velocity;
u = streamwise velocity at a point in the channel section;

$\mathbf{u}$ = streamwise velocity vector at a point in the channel section;
u_* = shear velocity;
V = mean cross-sectional velocity;
x = streamwise direction;
y = vertical direction;
z = lateral coordinate measured from the left bank of the stream;
z' = lateral coordinate measured from the wall of the left plate;
θ = angle between the positional vector and the boundary elemental vector;
κ = von Karman constant;
ν = kinematic viscosity;
ρ = mass density; and
τ_0 = boundary shear stress.

References

Chen, C. L. (1991). "Unified theory on power laws for flow resistance." *J. Hydraul. Eng.*, 117(3), 371–389.

Chen, Y. C., and Chiu, C. L. (2002). "An efficient method of discharge measurement in tidal streams." *J. Hydrol.*, 265, 212–224.

Dey, S., and Barbhuiya, A. K. (2005). "Flow field at a vertical-wall abutment." *J. Hydraul. Eng.*, 131(12), 1126–1135.

International Organization for Standardization. (1979). "Measurement of liquid flow in open channels-moving boat method." *Ref. No. ISO4369-1979(E)*, Geneva.

Kawanisi, K. (2004). "Structure of turbulent flow in a shallow tidal estuary." *J. Hydraul. Eng.*, 130(4), 360–370.

Kawanisi, K., Watanabe, S., Kaneko, A., and Abe, T. (2009). "River acoustic tomography for continuous measurement of water discharge." *Proc., 3rd Int. Conf. and Exhibition on Underwater Acoustic Measurements: Technologies and Results*, Nafplion, Greece, 613–620.

Lane, S. N., et al. (1998). "Three-dimensional measurement of river channel flow processes using acoustic doppler velocimetry." *Earth Surf. Processes Landforms*, 23(13), 1247–1267.

Lee, S., and Cheong, T. S. (2009). "Development of regression equations for the water discharge estimation in tidally effected rivers." *KSCE, J. Civil Engineering*, 13(3), 195–203.

Maghrebi, M. F. (2006). "Application of the single point measurement in discharge estimation." *Adv. Water Resour.*, 29, 1504–1514.

Maghrebi, M. F., and Ball, J. E. (2006). "New method for estimation of discharge." *J. Hydraul. Eng.*, 132(10), 1044–1051.

Maghrebi, M. F., and Rahimpour, M. (2005). "A simple model for estimation of dimensionless isovel contours in open channels." *Flow Meas. Instrum.*, 16, 347–352.

Rantz, S. E. (1983). "Measurement and computation of stream flow." *Computation of discharge. US Geology Survey, Water Supply, paper 2175*, Vol. 2, U.S. GPO, Washington, D.C.

Reichardt, H. (1956). "Über die Geschwindigkeitsverteilung in einer geradlinigen turbulenten Couette-Strömung (Velocity distribution in turbulent Couette-flow)." *ZAMM, Sonderheft*, 36, 26–29 (special issue).

Reichardt, H. (1959). "Gesetzmäßigkeiten der geradlinigen turbulenten Couette-Strömung (Governing roles in turbulet Couette-flow)." *Rep. No. 22*, Max-Planck-Inst. für Strömungsforschung and the Aerodyn. Versuchsanstalt, Göttingen, Germany.

Spurk, J. H. (1997). *Fluid mechanics, problems and solutions*, Springer, Berlin.

Tilley, J. H., Coates, A., Wojcik, A., Abustan, I., and Ball, J. E. (1999). "Gauging of rapidly varying flows in urban streams." *Proc., 8th Int. Conf. on Urban Storm Drainage*, Vol. 4, 1793–1699.

Yen, B. C. (2002). "Open channel flow resistance." *J. Hydraul. Eng.*, 128(1), 20–39.